

## Discovery of a Short-Period and Unusually Helium-Deficient Dwarf Nova KSP-OT-201701a by the KMTNet Supernova Program

YOUNGDAE LEE <sup>1,2</sup> SANG CHUL KIM <sup>2,3</sup> DAE-SIK MOON <sup>4</sup> HONG SOO PARK <sup>2,3</sup> MARIA R. DROUT <sup>4</sup>  
YUAN QI NI <sup>4</sup> AND HYOBIN IM <sup>2,3</sup>

<sup>1</sup>*Department of Astronomy and Space Science, Chungnam National University, Daejeon 34134, Republic of Korea*

<sup>2</sup>*Korea Astronomy and Space Science Institute, 776, Daedeokdae-ro, Yuseong-gu, Daejeon 34055, Republic of Korea*

<sup>3</sup>*Korea University of Science and Technology (UST), Daejeon 34113, Republic of Korea*

<sup>4</sup>*David A. Dunlap Department of Astronomy and Astrophysics, University of Toronto, 50 St. George Street, Toronto, ON M5S 3H4, Canada*

### ABSTRACT

We present the first ever discovery of a short-period and unusually helium-deficient dwarf nova KSP-OT-201701a by the Korea Microlensing Telescope Network Supernova Program. The source shows three superoutbursts, each led by a precursor outburst, and several normal outbursts in *BVI* during the span of  $\sim 2.6$  years with supercycle and normal cycle lengths of about 360 and 76 days, respectively. Spectroscopic observations near the end of a superoutburst reveal the presence of strong double-peaked H I emission lines together with weak He I emission lines. The helium-to-hydrogen intensity ratios measured by He I <sub>$\lambda$ 5876</sub> and H $\alpha$  lines are  $0.10 \pm 0.01$  at a quiescent phase and  $0.26 \pm 0.04$  at an outburst phase, similar to the ratios found in long-period dwarf novae while significantly lower than those in helium cataclysmic variables (He CVs). Its orbital period of  $51.91 \pm 2.50$  minutes, which is estimated based on time series spectroscopy, is a bit shorter than the superhump period of  $56.52 \pm 0.19$  minutes, as expected from the gravitational interaction between the eccentric disk and the secondary star. We measure its mass ratio to be  $0.37^{+0.32}_{-0.21}$  using the superhump period excess of  $0.089 \pm 0.053$ . The short orbital period, which is under the period minimum, the unusual helium deficiency, and the large mass ratio suggest that KSP-OT-201701a is a transition object evolving to a He CV from a long-period dwarf novae with an evolved secondary star.

*Keywords:* stars: dwarf novae — surveys — techniques: photometric — techniques: spectroscopic

### 1. INTRODUCTION

Dwarf novae are binary systems composed of a white dwarf (WD) as the primary and a low-mass star as the secondary (Warner 1995), accompanied by the accretion disk formed by mass-flow from the secondary. The increased temperature of the accretion disk resulting from mass accretion triggers outbursts that appear as dwarf novae (Cannizzo et al. 1986; Smak 1984; Osaki 1996). The evolution of dwarf novae is mainly determined by the loss of angular momentum driven by the gravitational radiation from their binary orbital motions (Paczynski & Sienkiewicz 1981; Rappaport et al. 1982). The orbital period and binary separation distance decrease as they evolve until they reach the so-called period minimum of about 80 minutes, at which point the gravitational radiation time scale becomes similar to the Kelvin-Helmholtz time scale. After the period minimum, the radius of the secondary star as well as the binary separation distance and orbital period start to increase, known as the periodic bouncer (Rappaport et al. 1982).

Of particular interests among dwarf novae is the origin and evolution of the small number of dwarf novae showing orbital periods below the period minimum. They occupy  $\sim 5\%$  of the entire population of dwarf novae (Pala et al. 2020), and are thought to have short periods because the increased density of the secondary resulting from the loss of an extended atmosphere shrinks the binary orbital motion (Podsiadlowski et al. 2003). This process is more effective

for an evolved secondary due to its already increased density near the center. The short-period dwarf novae are categorized into two subclasses: AM Canum Venaticorum (AM CVn) systems and He-rich cataclysmic variables (He CVs). The former show strong He emission with no H emission (Anderson et al. 2005), whereas the latter do both He and H emission together with a larger  $\text{He I}_{\lambda 5876}/\text{H}\alpha$  flux ratio (He/H; Kennedy et al. 2015). In comparison, dwarf novae above the period minimum show the flux ratio in the range of 0.15–0.30 (Williams & Ferguson 1982; Ritter & Kolb 2003; Thorstensen et al. 2004). The majority of the short-period dwarf novae are AM CVn systems, with He CVs being extremely rare and accounting for only  $\sim 7\%$  of them (Breedt et al. 2012).

Three different binary types have been suggested for the short-period dwarf novae: (1) binaries of two WDs; (2) binaries of a WD and a He-burning star with a stripped H envelope, and (3) binaries of a WD and an evolved star off the main sequence (see Green et al. 2020, and references therein). The first two types, which pass through two common envelope phases during their evolution, are known to be the origin of AM CVn showing no H emission. The third type, on the other hand, is known to be the origin of AM CVn and all of the He CVs (Podsiadlowski et al. 2003; Goliash & Nelson 2015; Green et al. 2020; El-Badry et al. 2021). According to Kennedy et al. (2015), a long-period binary composed of a WD and an evolved star off the main sequence very likely passes through a phase of He CV on its eventual evolution to an AM CVn by gradually losing H and showing higher He/H ratios as they evolve.

One of the key observations that can potentially confirm this evolution scenario of dwarf novae is the identification of an intermediate example that shows a short period but with a smaller He/H ratio than what has been observed in He CVs. To the best of our knowledge, no short-period dwarf nova below the period minimum has been observed with a He/H ratio  $< 0.5$ . In this *Letter*, we present the first discovery of which we name KSP-OT-201701a. We suggest that this object is most likely evolving from a long-period binary consisting of a WD and an evolved star to the short-period He CV phase.

## 2. DISCOVERY OF KSP-OT-201701a AND LIGHT CURVES

KSP-OT-201701a was discovered by the KMTNet (Korea Microlensing Telescope Network) Supernova Program (KSP; Moon et al. 2016) during its wide-field ( $= 2^\circ \times 2^\circ$  at a pixel sample rate of  $0''.4$  per pixel) monitoring observations of the spiral galaxy NGC 2280 for about 2.6 years between 2016 October and 2019 May. KSP conducts high-cadence, multi-color ( $= BVI$  bands) observations optimized for discovering and monitoring early supernovae (e.g., Afsariardchi et al. 2019; Moon et al. 2021), taking advantage of 24-hour continuous sky coverage provided by the three 1.6-m telescopes of the KMTNet (Kim et al. 2016) in Chile, South Africa and Australia. Such observations are also useful for understanding the origins and population of classical novae and dwarf novae (Antoniadis et al. 2017; Brown et al. 2018; Lee et al. 2019).

Figure 1 (top panel) shows the entire  $V$ -band light curve of KSP-OT-201701a, which is located at  $(\alpha, \delta)_{\text{J2000}} = (06^{\text{h}} 39^{\text{m}} 23.2^{\text{s}}, -26^\circ 37' 18.8'')$ <sup>1</sup>, obtained with the KMTNet. The integration time of each exposures is 60 seconds, and the mean cadence is about 8 hours for each of  $BVI$  bands. We use DAOPHOT-based point-spread function (PSF) photometry (DAOPHOT II; Stetson 1987) to obtain the fluxes of the source that were calibrated against nearby  $BVi'$  standard stars from the AAVSO Photometric All-Sky Survey database (APASS). We adopt the relation  $I = i' - 0.4$  to convert the APASS  $i'$ -band standard photometric system to the KMTNet  $I$ -band system (see Park et al. 2017, for the details). We apply the extinction correction of  $A_B = 0.51$  mag,  $A_V = 0.40$  mag, and  $A_I = 0.25$  mag using the extinction  $E(B - V) = 0.13$  mag toward KSP-OT-201701a in the Galactic extinction model of Schlegel et al. (1998) with the extinction reddening law of Cardelli et al. (1989) with  $R_V = 3.1$ . In this paper, we use extinction-corrected magnitudes and colors unless otherwise specified.

In the top panel of Figure 1, we can identify three apparent superoutbursts (which we call  $S1$ ,  $S2$ , and  $S3$ ) featured with the presence of a plateau of  $\sim 9$  days as shown in the bottom panel as well as six normal outbursts ( $N1$ – $N6$ ). We determine the mean quiescent magnitude of KSP-OT-201701a to be  $21.22 \pm 0.20$ ,  $21.11 \pm 0.20$ , and  $20.58 \pm 0.21$  mag in the  $B$ ,  $V$ , and  $I$  bands using the images obtained when there was no outburst activity. This gives a mean supercycle ( $P_{sc}$ ) period of 360 days for KSP-OT-201701a. However, considering the gap of the data when the source was near the Sun (green shades in the top panel of Figure 1), we note that we cannot rule out the possibility of  $P_{sc} = 180$  days. The mean cycle of normal outbursts is 78.5 days, indicating that there could be 4–5 normal outbursts between two superoutbursts, i.e.,  $N_{\text{nor}} = 4$ –5.

<sup>1</sup>  $(l, b) = (235.84662^\circ, -14.24921^\circ)$

We conduct polynomial fits to each light curve to estimate key light curve parameters of the outbursts in Figure 1 (see Lee et al. 2019, for example), such as peak magnitude, epoch of peak brightness, etc. As shown in the bottom panel of Figure 1 where each of the superoutbursts are aligned with respect to their respective peaks, the transition from the precursor to superoutburst occurs differently for each superoutburst, although they have very similar light curve shapes overall. The estimated outburst amplitude, duration as well as rising and decline rate of KSP-OT-201701a are comparable to those observed in SU UMa and U Gem dwarf novae sampled in Otulakowska-Hypka et al. (2016). Osaki (1996) classified the three (“active”, “intermediate”, “WZ Sge”) activity subgroups of SU UMa-type dwarf novae based on  $P_{sc}$  and  $N_{nor}$  which are related with mass-transfer rate. According to this classification,  $P_{sc}$  and  $N_{nor}$  of KSP-OT-201701a are similar to those of “active” SU UMa-type dwarf novae with a large mass-transfer rate.

SU UMa-type dwarf novae show superhumps, a periodic variation of brightness during superoutbursts, whose presence is often investigated using power spectrum analysis of the plateau phase (Kato et al. 2009). After the best-fit polynomial to each superoutburst light curve is subtracted out from the light curve, we combined residual light curves of the plateau phases (double arrow in the bottom panel of Figure 1) of the three superoutbursts in *BVI*. since the superhump periods of the plateau phases are known to be relatively invariant among different superoutbursts of the same object (Kato et al. 2009). With the combined residual light curve, we attempt to measure the superhump period ( $P_{sh}$ ) of KSP-OT-201701a using Lomb-Scargle analysis<sup>2</sup>.

Figure 2(a) shows the power spectrum of KSP-OT-201701a with three major powers at  $14.525 \pm 0.075$ ,  $22.475 \pm 0.075$ , and  $25.475 \pm 0.075$  cycle day<sup>-1</sup>, corresponding to  $99.14 \pm 0.19$ ,  $64.07 \pm 0.19$ , and  $56.52 \pm 0.19$  minutes, respectively. We note that all these three potential periods of KSP-OT-201701a are below the period gap (2h–3h) of dwarf novae (Otulakowska-Hypka et al. 2016), consistent with the postulation that KSP-OT-201701a is an SU UMa-type dwarf nova (Kato et al. 2009).

We also calculated the power spectrum with *BVI* light curves subtracted quiescent magnitudes in the quiescent phase between MJD of 57800 days and MJD of 57850 days. The results are shown in Figure 2(c). The significant peaks are populated around a frequency of 25 cycle day<sup>-1</sup>. This seems to imply that an orbital period of KSP-OT-201701a is around 58 minutes and the superhump period will be the similar value. Since, in Section 3, a spectroscopic orbital period is  $51.91 \pm 2.50$  minutes, the closest superhump period of  $56.52 \pm 0.19$  minutes from the spectroscopic orbital period is the most possible superhump period. Orbital phase diagram of the *V*-band for the orbital period of 51.91 minutes are shown in Figure 2(b).

### 3. SPECTROSCOPIC ANALYSIS: HELIUM TO HYDROGEN RATIO AND ORBITAL PERIOD

We conduct time series spectroscopic observations of KSP-OT-201701a using GMOS on the 8-m Gemini South telescope on 2018 February 9th around the end of the *S2* superoutburst as shown in Figure 1. We obtain 4 blue (3725Å–6770Å) and 4 red (5260Å–9860Å) GMOS spectra, each with an exposure time of 400 seconds, during about 1 hour. The spectral resolutions are FWHM = 2.73Å at 4610Å in the blue spectra and FWHM = 3.98Å at 7640Å in the red spectra. In addition, we make observations of the target using LDSS3-C on the 6.5-m Magellan Clay telescope on 2017 April 30th around the end of the *N2* normal outburst and we take two 1200-s exposures of LDSS3-C covering the spectral range of 4400Å–9990Å. The spectral resolution is FWHM = 8.25Å at 7100Å.

Figure 3 shows our stacked spectra of KSP-OT-201701a: gray color for the Gemini stacked spectrum and green color for the Magellan one. The overall continua of these spectra are almost same, but Gemini spectrum shows a flux excess below wavelength of 5500 Å. This seems to imply that Gemini spectrum is weakly affected by the outburst, while Magellan data is a quiescent spectrum. We identify strong Balmer emission lines alongside weak He I lines. The insets in Figure 3 are an enlarged spectrum around the H $\alpha$  and He I $_{\lambda 5876}$  lines, clearly revealing a double-peak structure of the line which is indicative of the presence of rotating accretion (Shafter 1983). We estimate the He to H line ratio (He/H) of KSP-OT-201701a using the He I $_{\lambda 5876}$  and the H $\alpha$  lines which have been used in Kennedy et al. (2015). The flux of the two emission lines are obtained after the underlying continuum emission is subtracted by a polynomial fit obtained from the line-free parts of the spectrum. The mean estimated He/H ratios in the eight individual GMOS spectra are  $0.18 \pm 0.08$  in the range of 0.07–0.29.

We use the radial velocity variations of the H $\alpha$  emission line in the eight GMOS time series spectra to estimate the orbital period of the primary of KSP-OT-201701a by applying the antisymmetric two Gaussian convolution technique (Shafter 1983) to the observed spectra in the range of 6500Å–6600Å. We fit the observed spectra of the H $\alpha$  lines in

<sup>2</sup> We use `astropy.stats.LombScargle` for this. (<http://docs.astropy.org/en/stable/stats/lombscargle.html>; Astropy Collaboration et al. 2013, 2018)

the eight Gemini spectra with  $13\text{\AA}$ – $21\text{\AA}$  for the range of the half separation distance between the two Gaussian peaks,  $10\text{\AA}$ – $50\text{\AA}$  for the range of the FWHM of the two Gaussians, and  $6500\text{\AA}$ – $6600\text{\AA}$  for the central wavelength range of the  $\text{H}\alpha$  line. We, then, adopt the circular orbit as following function

$$v(t) = \gamma + K \sin[2\pi(t - T_0)/P_{\text{orb}}] \quad (1)$$

where  $\gamma$ ,  $K$ ,  $T_0$ , and  $P_{\text{orb}}$  are the systematic velocity, semi-amplitude of radial velocity of the primary, time of the conjunction, and orbital period, respectively, for our fitting of the measured radial velocities of the  $\text{H}\alpha$  lines.

We followed the method in [Augustejn et al. \(1996\)](#) that determines the best-fit  $K$  and  $P_{\text{orb}}$  when the uncertainty to magnitude ratio ( $= \sigma_K/K$ ) of the parameter  $K$  is the minimum. We obtain the minimum  $\sigma_K/K$  when the separation of the two Gaussians in the  $\text{H}\alpha$  line is  $15.5\text{\AA}$ , and this gives the best-fit parameters  $\gamma = 38.5 \pm 12.4 \text{ km s}^{-1}$ ,  $K = 132.9 \pm 18.2 \text{ km s}^{-1}$ , and  $P_{\text{orb}} = 51.91 \pm 2.50$  minutes.

Figure 4 shows that the fitted circular orbit (red curve) of Equation (1) matches well the observed radial velocities (blue circles) of KSP-OT-201701a. In the figure, the first four spectra show the mean He/H ratio of  $\sim 0.12$ , while that of the next three is 0.26. We attribute the apparent systematic difference of the mean He/H ratio to the interference by the NaD ( $5890\text{\AA}$  and  $5896\text{\AA}$ ) from the cool secondary star to the broad  $\text{He I}_{\lambda 5876}$  line from the accretion disk when the secondary star is moving toward us in the first four spectra. The systematic difference in the line ratios between the first four and the next three spectra also supports the validity of our estimation of the orbital period of 51.91 minutes. Finally, we will adopt  $0.26 \pm 0.04$  as the uncontaminated He/H of KSP-OT-201701a. It should be noticed that He/H ratio measured from Gemini spectra could be affected by the superoutburst since we observed just before the end of the superoutburst (see Figure 1 and 3). It may make additional uncertainty about the measurement of He/H. Although it is difficult to measure this uncertainty, the measured He/H is probably weakly affected by outburst since a flux excess is weak above wavelength of  $5500\text{\AA}$  comparing a quiescent spectrum from the Magellan observations. In the case of a quiescent spectrum from Magellan, He/H ratio ( $0.10 \pm 0.01$ ) is quiet low. It seems that He emission line is partly contaminated by the NaD absorption since the exposures are three times longer (20 minutes) than those of the Gemini observations.

#### 4. DISCUSSION

In Figure 5, we compare the orbital period, He/H ratio, and mass ratio ( $q = M_2/M_1$ ) of KSP-OT-201701a (filled star) to those of He CVs (filled colored circles) of V485 Cen ([Augustejn et al. 1996](#); [Olech 1997](#)), EI Psc ([Thorstensen et al. 2002](#)), OV Boo ([Patterson et al. 2008](#)), CSS 100603 ([Breedt et al. 2012](#); [Kato et al. 2010](#)), CSS 120422 ([Carter et al. 2013](#)), and V418 Ser ([Green et al. 2020](#); [Kennedy et al. 2015](#)) and long-period dwarf novae (red squares; [Williams & Ferguson 1982](#); [Ritter & Kolb 2003](#); [Thorstensen et al. 2004](#)). They represent the entire sample of the He CVs and long-period dwarf novae observed with these parameters available in literature to the best of our knowledge. Among the short-period dwarf novae, KSP-OT-201701a in Figure 5(a) appears to have the lowest He/H ratio of 0.10–0.26 among the short-period dwarf novae (i.e., He CVs and AM CVn) and it is similar to the ratios typically observed in long-period dwarf novae (see Section 3). According to binary population synthesis models ([Podsiadlowski et al. 2003](#); [Goliash & Nelson 2015](#)), a long-period dwarf nova with an evolved secondary and a low central hydrogen fraction  $X_c \lesssim 0.1$  evolves to He CVs as its orbital period and mass ratio decrease. This indicates that KSP-OT-201701a is an intermediate stage between long-period dwarf novae and He CVs.

The superhump period excess, i.e.,  $\epsilon = P_{sh}/P_{orb} - 1$ , can be derived from the precession of the eccentric disk of a dwarf nova caused by the secondary star perturbation, dependent on the mass ratio of the system ([Whitehurst 1988](#); [Lubow 1991](#); [Hirose & Osaki 1990](#); [Patterson 2001](#); [Patterson et al. 2005](#); [Knigge 2006](#)). We follow three empirical relations between the period excess and mass ratio of dwarf novae ([Patterson 2001](#); [Patterson et al. 2005](#); [Knigge 2006](#)) to estimate the mass ratio of KSP-OT-201701a to be  $0.32_{-0.17}^{+0.46}$ ,  $0.37_{-0.21}^{+0.23}$ , and  $0.41_{-0.24}^{+0.27}$ . As shown in Figure 5(b), the mass ratios of long-period dwarf novae are in the range of 0.207–0.941 with an average of 0.523, whereas those of He CVs are in the range of 0.017–0.384 with an average of 0.148. The mass ratio of KSP-OT-201701a is comparable with what is typically found in long-period dwarf novae, but it is very similar to the largest ratio found in He CVs.

The dashed red lines in Figure 5 show the potential evolutionary track of KSP-OT-201701a from a long-period dwarf nova with an evolved secondary to a He CV as observed today ([Podsiadlowski et al. 2003](#); [Kennedy et al. 2015](#)). During the previous evolution to the current He CV phase, the mass ratio and orbital period of KSP-OT-201701a have decreased due to the mass loss of the secondary and the angular momentum loss of the binary system to reach the current orbital period of  $\sim 52$  minutes below the period minimum. It is highly likely that KSP-OT-201701a is in an

early phase of a He CV given its small He/H ratio and large mass ratio, having lost only part of its hydrogen envelope so far. We expect KSP-OT-201701a to continuously lose its hydrogen envelope, progressively revealing its helium envelope with an increasing He/H ratio, as commonly observed in He CVs before they become AM CVn. The expected sudden increase of He/H ratio deep inside a low mass star as a result of nucleosynthesis (see Boehm-Vitense 1992) leads to the large He/H ratio observed in He CVs as the secondaries keep losing their hydrogen envelopes (Schenker et al. 2002).

## 5. SUMMARY AND CONCLUSION

We discovered for the first time a short-period and unusually helium-deficient dwarf nova (KSP-OT-201701a). We summarize and conclude our results as follows.

- KSP-OT-201701a has shown rich features of outbursts of a dwarf nova, including normal outbursts and super-outbursts with precursors. In terms of superoutburst cycle ( $P_{sc}$ ) and the number of normal outbursts ( $N_{nor}$ ), KSP-OT-201701a has similar features of the "active" subgroup of SU UMa dwarf novae with large mass-transfer rate.
- We determine the orbital period of KSP-OT-201701a to be 51.91 minutes based on our time-series spectroscopic observations and the period of superhumps to be  $56.52 \pm 0.19$  minutes during the plateau of superoutbursts. The superhump period excess is large ( $0.089 \pm 0.053$ ), compatible with a mass ratio ( $M_2/M_1$ ) of  $0.37^{+0.32}_{-0.21}$ .
- The observed flux ratios ( $\text{He I}_{\lambda 5876}/\text{H}\alpha = 0.10 \pm 0.01$  at a quiescent phase and  $0.26 \pm 0.04$  at an outburst phase) of KSP-OT-201701a are similar to those of dwarf novae with a long ( $> 80$  minutes) period, and is the lowest value among He CVs.
- We suggest that the short-period and unusually helium-deficient nature of KSP-OT-201701a is consistent with a dwarf nova in an intermediate stage evolving into a He CV from a long-period dwarf nova with an evolved secondary star.

This research has made use of the KMTNet facility operated by the Korea Astronomy and Space Science Institute, and the data were obtained at the three host sites of CTIO in Chile, SAAO in South Africa, and SSO in Australia. YDL acknowledges support from Basic Science Research Program through the National Research Foundation of Korea (NRF) funded by the Ministry of Education (2020R1A6A3A01099777). DSM was supported in part by a Leading Edge Fund from the Canadian Foundation for Innovation (project No. 30951) and a Discovery Grant (RGPIN-2019-06524) from the Natural Sciences and Engineering Research Council (NSERC) of Canada. HSP was supported in part by the National Research Foundation of Korea (NRF) grant funded by the Korea government (MSIT, Ministry of Science and ICT; No. NRF-2019R1F1A1058228). MRD acknowledges support from NSERC through grant RGPIN-2019-06186, the Canada Research Chairs Program and the Canadian Institute for Advanced Research.

## REFERENCES

- Afsariardchi, N., Moon, D.-S., Drout, M. R., et al. 2019, ApJ, 881, 22, doi: [10.3847/1538-4357/ab2be6](https://doi.org/10.3847/1538-4357/ab2be6)
- Anderson, S. F., Haggard, D., Homer, L., et al. 2005, AJ, 130, 2230, doi: [10.1086/491587](https://doi.org/10.1086/491587)
- Antoniadis, J., Moon, D.-S., Ni, Y. Q., et al. 2017, ApJ, 844, 160, doi: [10.3847/1538-4357/aa706b](https://doi.org/10.3847/1538-4357/aa706b)
- Astropy Collaboration, Robitaille, T. P., Tollerud, E. J., et al. 2013, A&A, 558, A33, doi: [10.1051/0004-6361/201322068](https://doi.org/10.1051/0004-6361/201322068)
- Astropy Collaboration, Price-Whelan, A. M., Sipőcz, B. M., et al. 2018, AJ, 156, 123, doi: [10.3847/1538-3881/aabc4f](https://doi.org/10.3847/1538-3881/aabc4f)
- Augusteijn, T., van der Hooft, F., de Jong, J. A., & van Paradijs, J. 1996, A&A, 311, 889
- Boehm-Vitense, E. 1992, Introduction to Stellar Astrophysics. Vol.3: Stellar structure and evolution
- Breedt, E., Gänsicke, B. T., Marsh, T. R., et al. 2012, MNRAS, 425, 2548, doi: [10.1111/j.1365-2966.2012.21724.x](https://doi.org/10.1111/j.1365-2966.2012.21724.x)
- Brown, S., Moon, D.-S., Ni, Y. Q., et al. 2018, ApJ, 860, 21, doi: [10.3847/1538-4357/aabfe2](https://doi.org/10.3847/1538-4357/aabfe2)
- Cannizzo, J. K., Wheeler, J. C., & Polidan, R. S. 1986, ApJ, 301, 634, doi: [10.1086/163929](https://doi.org/10.1086/163929)

- Cardelli, J. A., Clayton, G. C., & Mathis, J. S. 1989, *ApJ*, 345, 245, doi: [10.1086/167900](https://doi.org/10.1086/167900)
- Carter, P. J., Steeghs, D., de Miguel, E., et al. 2013, *MNRAS*, 431, 372, doi: [10.1093/mnras/stt169](https://doi.org/10.1093/mnras/stt169)
- El-Badry, K., Rix, H.-W., Quataert, E., Kupfer, T., & Shen, K. J. 2021, *MNRAS*, 508, 4106, doi: [10.1093/mnras/stab2583](https://doi.org/10.1093/mnras/stab2583)
- Goliashch, J., & Nelson, L. 2015, *ApJ*, 809, 80, doi: [10.1088/0004-637X/809/1/80](https://doi.org/10.1088/0004-637X/809/1/80)
- Green, M. J., Marsh, T. R., Carter, P. J., et al. 2020, *MNRAS*, 496, 1243, doi: [10.1093/mnras/staa1509](https://doi.org/10.1093/mnras/staa1509)
- Hirose, M., & Osaki, Y. 1990, *PASJ*, 42, 135
- Kato, T., Imada, A., Uemura, M., et al. 2009, *PASJ*, 61, S395, doi: [10.1093/pasj/61.sp2.S395](https://doi.org/10.1093/pasj/61.sp2.S395)
- Kato, T., Maehara, H., Uemura, M., et al. 2010, *PASJ*, 62, 1525, doi: [10.1093/pasj/62.6.1525](https://doi.org/10.1093/pasj/62.6.1525)
- Kennedy, M., Garnavich, P., Callanan, P., et al. 2015, *ApJ*, 815, 131, doi: [10.1088/0004-637X/815/2/131](https://doi.org/10.1088/0004-637X/815/2/131)
- Kim, S.-L., Lee, C.-U., Park, B.-G., et al. 2016, *Journal of Korean Astronomical Society*, 49, 37, doi: [10.5303/JKAS.2016.49.1.037](https://doi.org/10.5303/JKAS.2016.49.1.037)
- Knigge, C. 2006, *MNRAS*, 373, 484, doi: [10.1111/j.1365-2966.2006.11096.x](https://doi.org/10.1111/j.1365-2966.2006.11096.x)
- Lee, Y., Moon, D.-S., Kim, S. C., et al. 2019, *ApJ*, 880, 109, doi: [10.3847/1538-4357/ab2985](https://doi.org/10.3847/1538-4357/ab2985)
- Lubow, S. H. 1991, *ApJ*, 381, 268, doi: [10.1086/170648](https://doi.org/10.1086/170648)
- Moon, D.-S., Kim, S. C., Lee, J.-J., et al. 2016, in *Proc. SPIE*, Vol. 9906, Ground-based and Airborne Telescopes VI, 99064I, doi: [10.1117/12.2233921](https://doi.org/10.1117/12.2233921)
- Moon, D.-S., Ni, Y. Q., Drout, M. R., et al. 2021, *ApJ*, 910, 151, doi: [10.3847/1538-4357/abe466](https://doi.org/10.3847/1538-4357/abe466)
- Olech, A. 1997, *AcA*, 47, 281. <https://arxiv.org/abs/astro-ph/9706180>
- Osaki, Y. 1996, *PASP*, 108, 39, doi: [10.1086/133689](https://doi.org/10.1086/133689)
- Otulakowska-Hypka, M., Olech, A., & Patterson, J. 2016, *MNRAS*, 460, 2526, doi: [10.1093/mnras/stw1120](https://doi.org/10.1093/mnras/stw1120)
- Paczynski, B., & Sienkiewicz, R. 1981, *ApJL*, 248, L27, doi: [10.1086/183616](https://doi.org/10.1086/183616)
- Pala, A. F., Gänsicke, B. T., Breedt, E., et al. 2020, *MNRAS*, 494, 3799, doi: [10.1093/mnras/staa764](https://doi.org/10.1093/mnras/staa764)
- Park, H. S., Moon, D.-S., Zaritsky, D., et al. 2017, *ApJ*, 848, 19, doi: [10.3847/1538-4357/aa88ab](https://doi.org/10.3847/1538-4357/aa88ab)
- Patterson, J. 2001, *PASP*, 113, 736, doi: [10.1086/320810](https://doi.org/10.1086/320810)
- Patterson, J., Thorstensen, J. R., & Knigge, C. 2008, *PASP*, 120, 510, doi: [10.1086/588615](https://doi.org/10.1086/588615)
- Patterson, J., Kemp, J., Harvey, D. A., et al. 2005, *PASP*, 117, 1204, doi: [10.1086/447771](https://doi.org/10.1086/447771)
- Podsiadlowski, P., Han, Z., & Rappaport, S. 2003, *MNRAS*, 340, 1214, doi: [10.1046/j.1365-8711.2003.06380.x](https://doi.org/10.1046/j.1365-8711.2003.06380.x)
- Rappaport, S., Joss, P. C., & Webbink, R. F. 1982, *ApJ*, 254, 616, doi: [10.1086/159772](https://doi.org/10.1086/159772)
- Ritter, H., & Kolb, U. 2003, *A&A*, 404, 301, doi: [10.1051/0004-6361:20030330](https://doi.org/10.1051/0004-6361:20030330)
- Schenker, K., King, A. R., Kolb, U., Wynn, G. A., & Zhang, Z. 2002, *MNRAS*, 337, 1105, doi: [10.1046/j.1365-8711.2002.05999.x](https://doi.org/10.1046/j.1365-8711.2002.05999.x)
- Schlegel, D. J., Finkbeiner, D. P., & Davis, M. 1998, *ApJ*, 500, 525, doi: [10.1086/305772](https://doi.org/10.1086/305772)
- Shafter, A. W. 1983, *ApJ*, 267, 222, doi: [10.1086/160861](https://doi.org/10.1086/160861)
- Smak, J. 1984, *PASP*, 96, 5, doi: [10.1086/131295](https://doi.org/10.1086/131295)
- Stetson, P. B. 1987, *PASP*, 99, 191, doi: [10.1086/131977](https://doi.org/10.1086/131977)
- Thorstensen, J. R., Fenton, W. H., Patterson, J. O., et al. 2002, *ApJL*, 567, L49, doi: [10.1086/339905](https://doi.org/10.1086/339905)
- Thorstensen, J. R., Fenton, W. H., & Taylor, C. J. 2004, *PASP*, 116, 300, doi: [10.1086/382792](https://doi.org/10.1086/382792)
- Warner, B. 1995, *Cambridge Astrophysics Series*, 28
- Whitehurst, R. 1988, *MNRAS*, 232, 35, doi: [10.1093/mnras/232.1.35](https://doi.org/10.1093/mnras/232.1.35)
- Williams, R. E., & Ferguson, D. H. 1982, *ApJ*, 257, 672, doi: [10.1086/160022](https://doi.org/10.1086/160022)

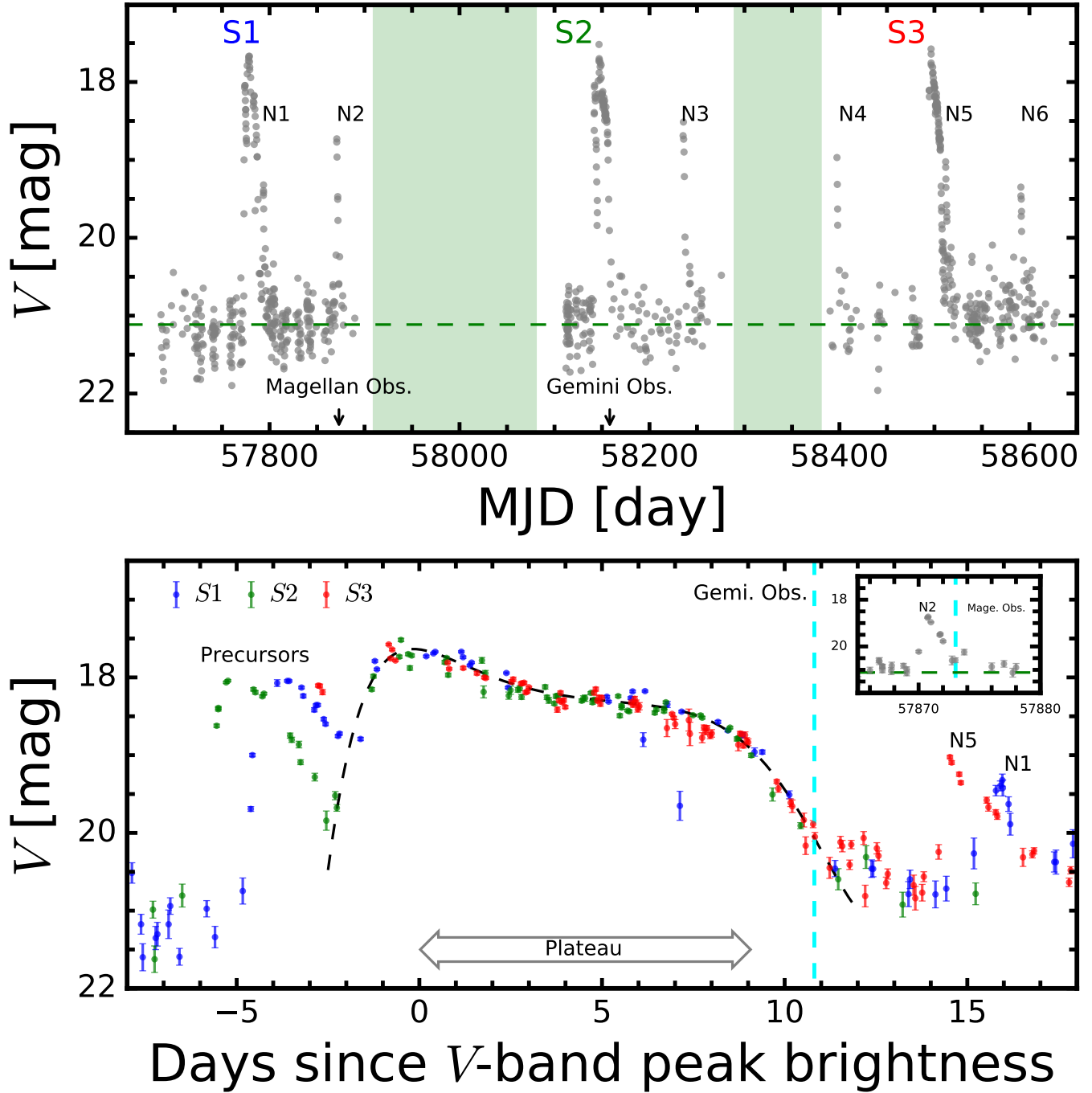


**Figure 1.** (*Top Panel*) The observed  $V$ -band light curve of KSP-OT-201701a for  $\sim 2.6$  years showing three superoutbursts (S1–S3) as well as six normal outbursts (N1–N6). The horizontal dashed line represents the mean quiescent magnitude  $V = 21.11$  mag. Two arrows indicate the epoch of spectroscopic observations. Green shades represent the epochs when the source was near the Sun. (*Bottom Panel*) Three superoutbursts S1 (blue dots), S2 (green dots), and S3 (red dots) are compared with the best-fit polynomial (black dashed line). Their plateau duration is indicated by the double arrow. (*Inset Panel*) The observed  $V$ -band light curve for N2 is shown. The vertical dashed lines indicate the epoch of spectroscopic observations.

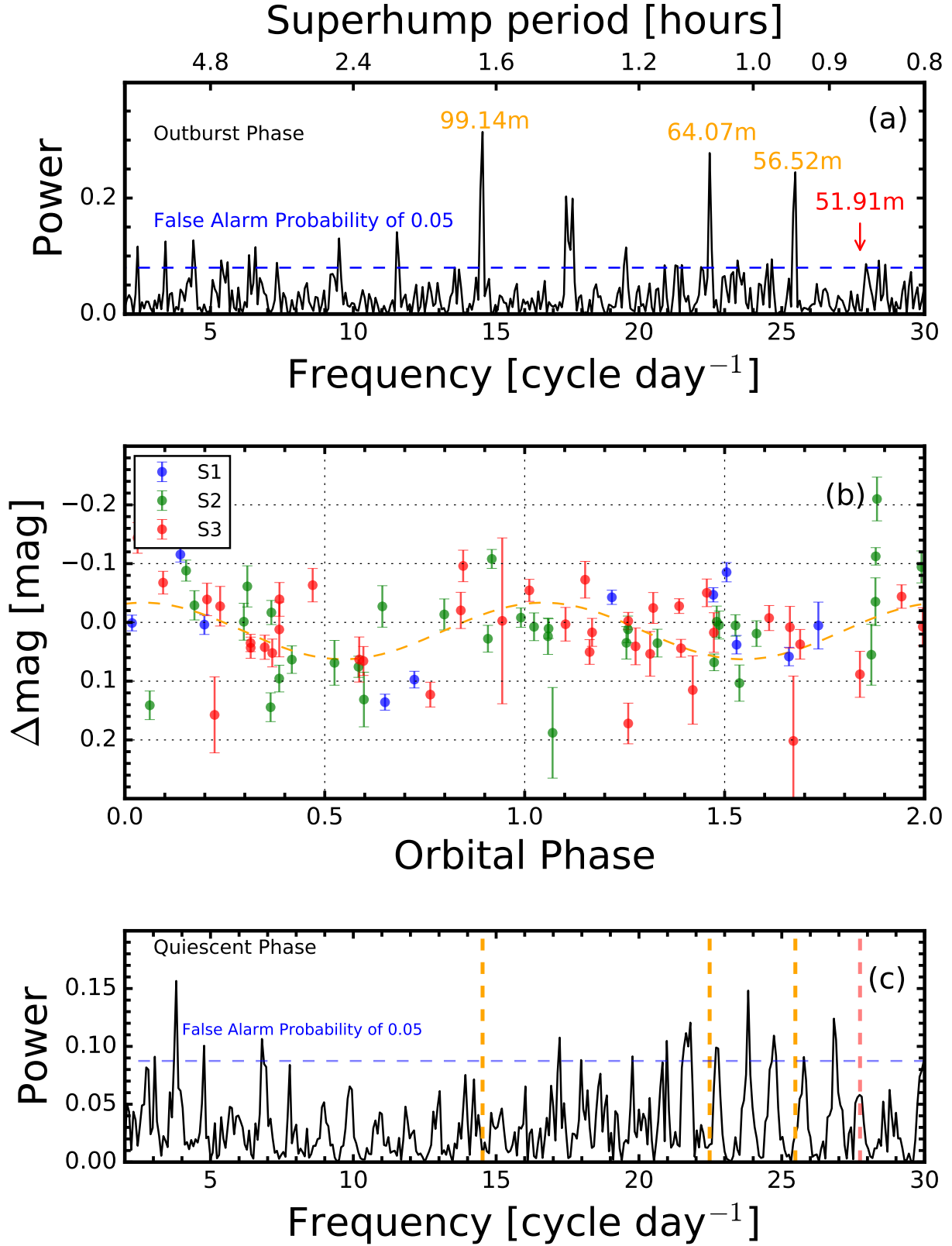


**Figure 2.** (a) Power spectrum of superhump of KSP-OT-201701a from Lomb-Scargle Periodogram analysis of the combined light curve of the three superoutbursts in *BVI*. The horizontal dashed line is a false alarm probability of 0.05. Red arrow indicates the orbital period measured from the spectroscopic data. (b) Orbital phase diagram of the *V*-band residuals obtained after subtracting the polynomial fit from the observed light curves in Figure 1 (bottom panel). We used the orbital period of 51.91 minutes. (c) Power spectrum in quiescent phase of KSP-OT-201701a with the combined light curves between MJD of 57800 days and 57850 days in *BVI*. The horizontal dashed line is a false alarm probability of 0.05. Four vertical dashed lines from left to right are 14.525, 22.475, 25.475 and 27.740 cycle day<sup>-1</sup>.



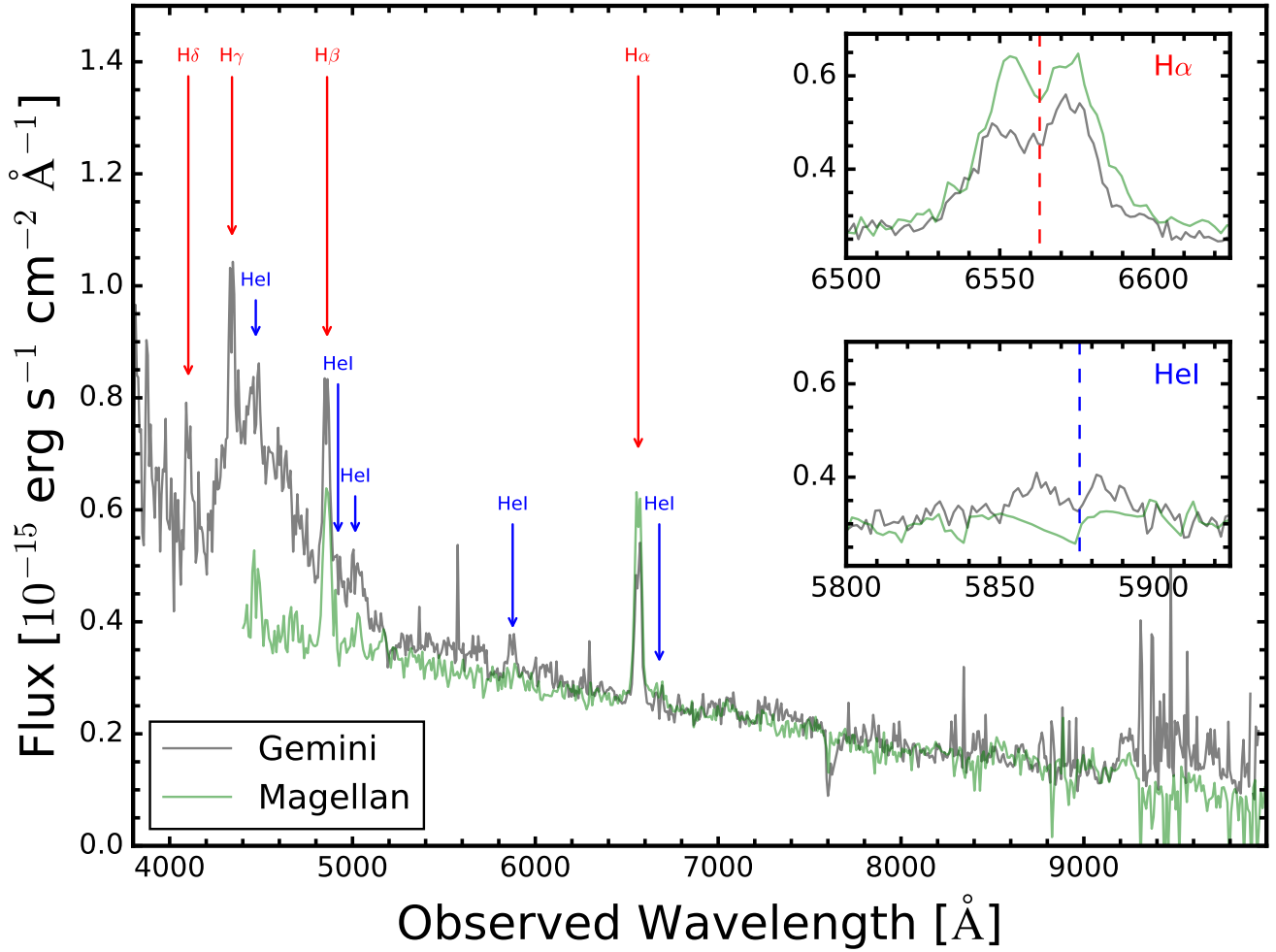


**Figure 3.** Stacked Gemini (gray) and Magellan (green) spectra of KSP-OT-201701a. The identified Hydrogen and Helium emission lines are denoted by the arrows. The inset panels give a magnified view of the  $H\alpha$  and the  $He\text{I}$  line, respectively, confirming its double-peaked structure. The Magellan spectrum was obtained when the source was fainter than the epoch of Gemini observations, and is shifted upward to match the continuum level of the Gemini spectrum.

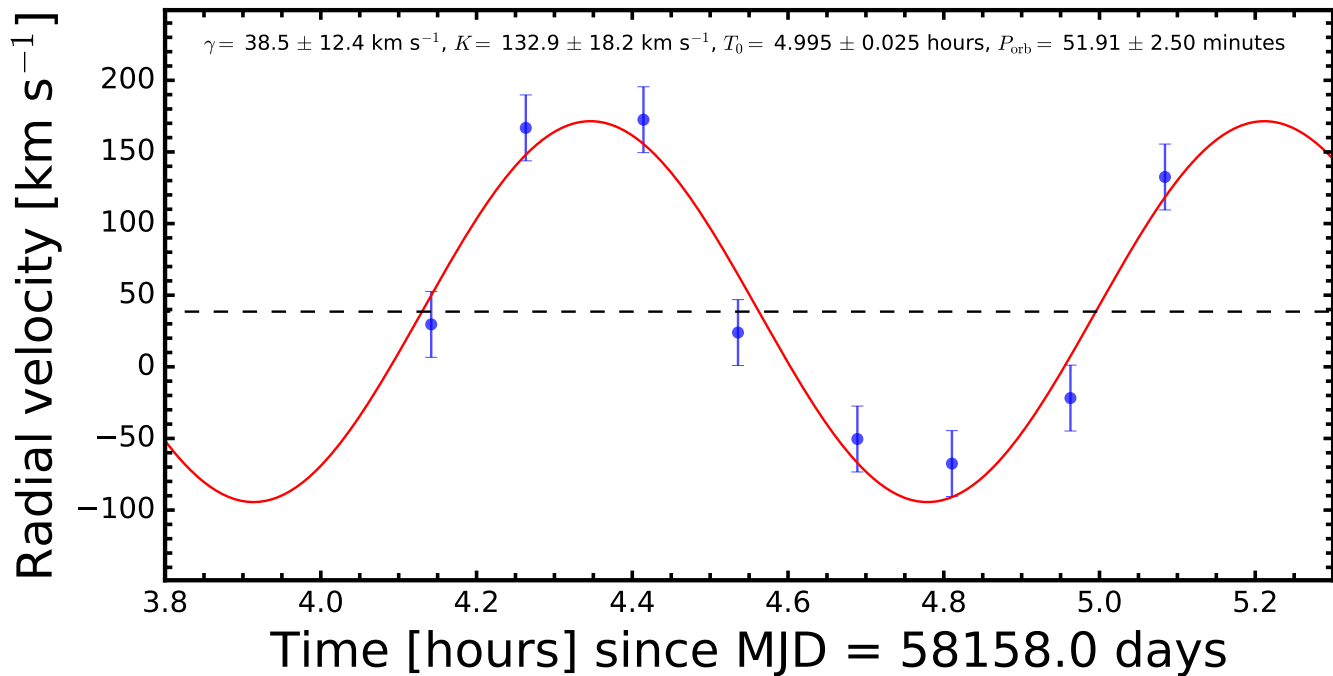


**Figure 4.** Observed radial velocity (blue circles) sequence of H $\alpha$  line from the Gemini spectra. The red curve represents the best-fit orbital velocity. The dashed line is the systematic velocity of the binary. Uncertainties of radial velocity at each epoch are the interval ( $0.5\text{\AA}$ ) of the half separation distance ( $a$ ) which is converted to  $23$  km s $^{-1}$  at  $6563\text{\AA}$ .

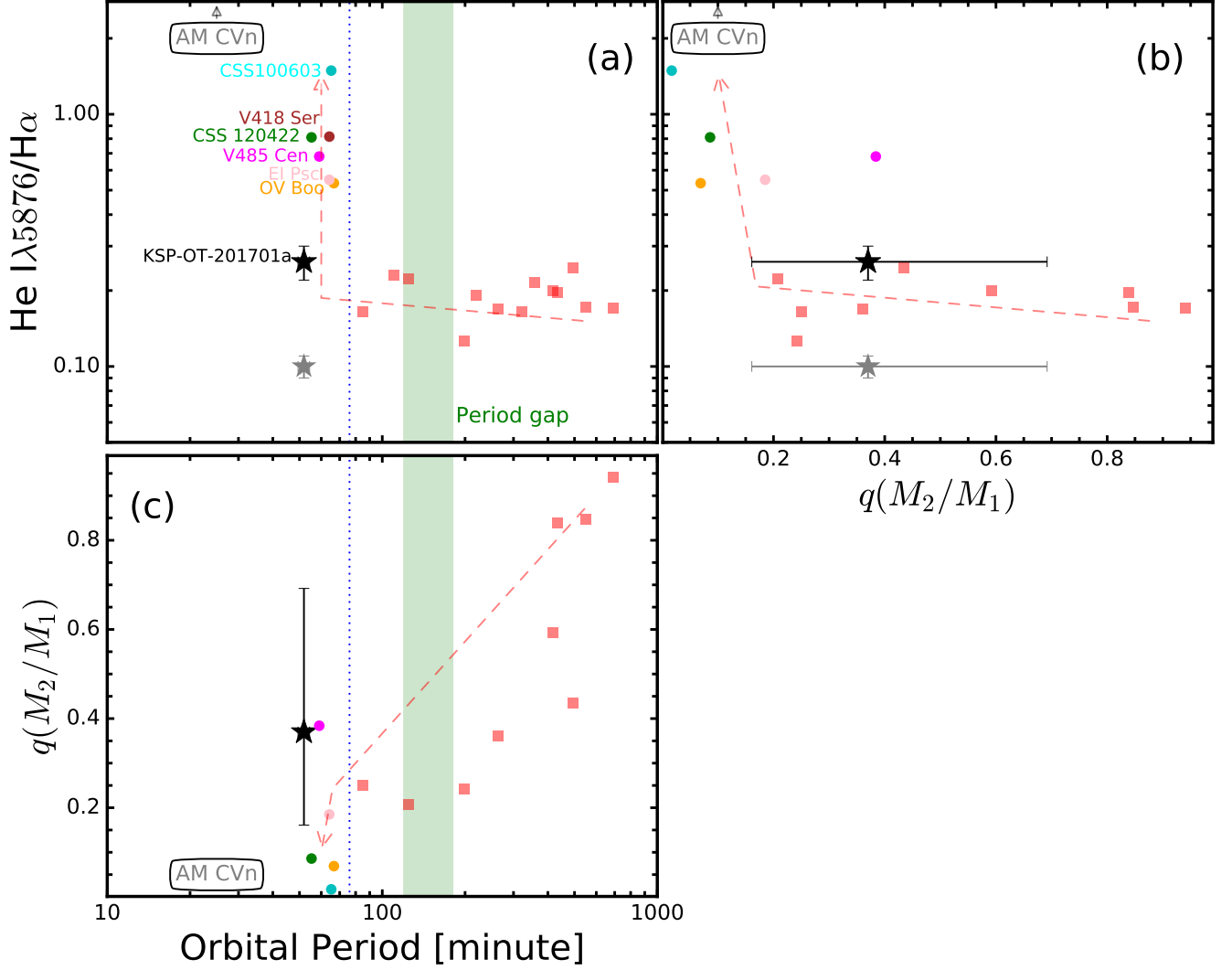


**Figure 5.** Comparisons of the orbital periods, He/H, and mass ratio  $q(M_2/M_1)$  of short-period dwarf novae (colored filled circles), long-period dwarf novae (red squares), and KSP-OT-201701a at an outburst (black star) and a quiescent phase (gray star) : (a) Orbital periods vs. He/H ratios; (b) mass ratios vs. He/H ratios; (c) orbital periods vs. mass ratios. Mass ratio is a mean value measured by the three empirical relations. The green shaded area and the blue dotted vertical lines in (a) and (c) are the period gap between 2 and 3 hours and the period minimum of 76 minutes, respectively. The red dashed lines with an arrow in (a)–(c) roughly represent the expected evolutionary paths of a dwarf nova with an evolved secondary, as its orbital period decreases as a result of mass loss. The locations of AM CVn, which are a group of dwarf novae with small orbital periods, small mass ratio, and no H emission, are shown in (a)–(c). See Section 4 for the references of the dwarf novae shown here.